

NASA/TM—2006-214110



Tensile and Creep Property Characterization of Potential Brayton Cycle Impeller and Duct Materials

Timothy P. Gabb and John Gayda
Glenn Research Center, Cleveland, Ohio

February 2006

The NASA STI Program Office . . . in Profile

Since its founding, NASA has been dedicated to the advancement of aeronautics and space science. The NASA Scientific and Technical Information (STI) Program Office plays a key part in helping NASA maintain this important role.

The NASA STI Program Office is operated by Langley Research Center, the Lead Center for NASA's scientific and technical information. The NASA STI Program Office provides access to the NASA STI Database, the largest collection of aeronautical and space science STI in the world. The Program Office is also NASA's institutional mechanism for disseminating the results of its research and development activities. These results are published by NASA in the NASA STI Report Series, which includes the following report types:

- **TECHNICAL PUBLICATION.** Reports of completed research or a major significant phase of research that present the results of NASA programs and include extensive data or theoretical analysis. Includes compilations of significant scientific and technical data and information deemed to be of continuing reference value. NASA's counterpart of peer-reviewed formal professional papers but has less stringent limitations on manuscript length and extent of graphic presentations.
- **TECHNICAL MEMORANDUM.** Scientific and technical findings that are preliminary or of specialized interest, e.g., quick release reports, working papers, and bibliographies that contain minimal annotation. Does not contain extensive analysis.
- **CONTRACTOR REPORT.** Scientific and technical findings by NASA-sponsored contractors and grantees.

- **CONFERENCE PUBLICATION.** Collected papers from scientific and technical conferences, symposia, seminars, or other meetings sponsored or cosponsored by NASA.
- **SPECIAL PUBLICATION.** Scientific, technical, or historical information from NASA programs, projects, and missions, often concerned with subjects having substantial public interest.
- **TECHNICAL TRANSLATION.** English-language translations of foreign scientific and technical material pertinent to NASA's mission.

Specialized services that complement the STI Program Office's diverse offerings include creating custom thesauri, building customized databases, organizing and publishing research results . . . even providing videos.

For more information about the NASA STI Program Office, see the following:

- Access the NASA STI Program Home Page at <http://www.sti.nasa.gov>
- E-mail your question via the Internet to help@sti.nasa.gov
- Fax your question to the NASA Access Help Desk at 301-621-0134
- Telephone the NASA Access Help Desk at 301-621-0390
- Write to:
NASA Access Help Desk
NASA Center for Aerospace Information
7121 Standard Drive
Hanover, MD 21076



Tensile and Creep Property Characterization of Potential Brayton Cycle Impeller and Duct Materials

Timothy P. Gabb and John Gayda
Glenn Research Center, Cleveland, Ohio

National Aeronautics and
Space Administration

Glenn Research Center

Trade names or manufacturers' names are used in this report for identification only. This usage does not constitute an official endorsement, either expressed or implied, by the National Aeronautics and Space Administration.

Available from

NASA Center for Aerospace Information
7121 Standard Drive
Hanover, MD 21076

National Technical Information Service
5285 Port Royal Road
Springfield, VA 22100

Available electronically at <http://gltrs.grc.nasa.gov>

Tensile and Creep Property Characterization of Potential Brayton Cycle Impeller and Duct Materials

Timothy P. Gabb and John Gayda
National Aeronautics and Space Administration
Glenn Research Center
Cleveland, Ohio 44135

Abstract

This paper represents a status report documenting the work on creep of superalloys performed under Project Prometheus. Cast superalloys have potential applications in space as impellers within closed-loop Brayton cycle nuclear power generation systems. Likewise wrought superalloys are good candidates for ducts and heat exchangers transporting the inert working gas in a Brayton-based power plant. Two cast superalloys, Mar-M247LC and IN792, and a NASA Glenn Research Center powder metallurgy superalloy, LSHR, are being screened to compare their respective capabilities for impeller applications. Several wrought superalloys including Hastelloy X (Haynes International, Inc., Kokomo, IN), Inconel 617, Inconel 740, Nimonic 263, and Incoloy MA956 (Special Metals Corporation, Huntington, WV), are also being screened to compare their capabilities for duct applications. These proposed applications would require sufficient strength and creep resistance for long term service at temperatures up to 1200 K, with service times to 100,000 h or more. Conventional tensile and creep tests were performed at temperatures up to 1200 K on specimens extracted from the materials. Initial microstructure evaluations were also undertaken.

Introduction

Certain space operations require an electric power source that is not dependent on the sun and can perform for long time periods. A promising concept fulfilling these requirements uses a nuclear reactor to heat an inert He-Xe working gas, which is expanded in a closed-loop Brayton cycle to power a turbo-generator for electricity production (ref. 1). There are multiple combinations of reactor and heat exchanger design that can be used, but in each scenario power conversion efficiency increases with higher turbine temperature. Also space power systems may be required to operate for very long service times. In the Jupiter Icy Moons Orbiter (JIMO) vehicle concept, the turbo-generator would require an impeller (radial turbine wheel) which can operate with sustained centrifugal loads for times extending to 100,000 h and maximum temperatures approaching 1200 K. Cast superalloys such as Mar-M247LC and IN792 could potentially be used for these impellers, provided creep and alloy phase stability are sufficient. LSHR is an advanced powder metallurgy superalloy that could also have potential for these impellers, offering higher strength and fatigue resistance but somewhat lower temperature capability.

Ducts subjected to pressure and thermal loads at similar temperatures will be needed to route and cool the working gas (ref. 2). The associated materials will need to be shaped, brazed, and welded into duct and turbine housing components. Solid solution strengthened wrought superalloys such as Hastelloy X, and Inconel 617 could be readily fabricated in these ways. However, their high temperature creep resistance may be insufficient. Precipitation hardened wrought superalloys such as Nimonic 263 and Inconel 740 have improved creep resistance, but could be harder to shape, join, and subsequently precipitation heat treat. Mechanically alloyed, precipitation hardened wrought superalloys such as Incoloy MA956 can have even higher creep resistance at high temperatures near 1200 K, but are very difficult to shape and join. Long term creep tests are therefore needed at realistic stresses and temperatures to compare these alloys at simulated the service conditions.

The objective of this study was to begin screening the mechanical properties of these materials for potential space applications. Potential impeller alloys Mar-M247LC, IN792, and LSHR, and potential

duct alloys Hastelloy X, Inconel 617, Inconel 740, Nimonic 263, and Incoloy MA956 were screened with selective tensile and creep testing. Typical material data bases do not include creep tests beyond about 10,000 h or consider such long term exposure in inert gases (ref. 3). Based on the long durations envisioned in some of these space applications, short term creep tests are being run in order to enable selection of allowable creep stresses and temperatures conducive to such long durations. Some of these tests are still ongoing, but results generated to date will be reviewed.

Materials and Procedure

Impeller Materials

Most Mar-M247LC (ref. 4) bars were cast at PCC, Inc. in a 1 by 18 bar mold using standard foundry practices. Additional bars were cast using the Microcast process to produce finer grain size. The bars had diameters about 1.9 cm and lengths of about 15 cm. These bars were subsequently hot isostatically pressed at 1458 K using a pressure of 172 MPa for 4 h. They were then solution heat treated in a vacuum furnace at 1494 K/2 h/Argon quench, and aged at 1352 K/4 h/Argon quench + 1144 K/20 h/air quench. An impeller from an auxiliary power unit of the superalloy IN792 (ref. 5) was provided by Sundstrand Aerospace. It had been cast using the Grainex process, another fine grain casting process, at Howmet. It was then hot isostatically pressed and heat treated using proprietary processes. Powder of LSHR superalloy (ref. 6) was atomized by Special Metals Corp. in argon and passed through screens of –270 mesh to give powder particle diameters of no more than about 55 μm . The powder was then sealed in a stainless steel container, hot compacted, and extruded at a reduction ratio of 6:1. Segments of the extrusion billet were machined into sections 15 cm in diameter and 20 cm long, then isothermally forged into a flat disk about 30 cm in diameter and 4 cm thick by Wyman-Gordon Forgings. The disk was solution heat treated at about 1444 K for 2.5 h, then transferred in 2 min for a quench in air by fans on each side of the disk. The disk was then given an aging heat treatment of 1128 K/8 h.

Duct Materials

Most of the wrought alloys were supplied by Special Metals Corp. Hot rolled plates of Hastelloy X (refs. 7 and 8), Inconel 617 (ref. 9), and Incoloy MA956 (ref. 10) of about 0.64 cm in thickness were supplied. They had been given a solution annealing heat treatment, and were tested in this state. A hot rolled plate of Inconel 740 (refs. 11 and 12) plate of 1.6 cm thickness and a Nimonic 263 (ref. 13) section of 4 cm thickness were also supplied in solution annealed and air quenched form. Unlike the other wrought duct materials, Inconel 740 and Nimonic 263 require an aging heat treatment in order to precipitate strengthening γ' precipitates. Therefore, they were subsequently given an aging heat treatment of 1073 K/8 h before testing.

Testing

Microstructure.—Actual compositions of the test materials were measured using inductively coupled plasma spectroscopy. Grain sizes were determined from metallographically prepared grip sections of tensile specimens according to ASTM E112 linear intercept procedures using circular grid overlays, and As-Large-As (ALA) grain sizes were determined using ASTM E930.

Creep Tests.—Machining of creep specimens was performed by Metcut Research Associates. Creep specimens with a gage diameter of 0.63 cm and gage length of 3.8 cm were machined from the candidate impeller materials. Smaller creep specimens with a gage diameter of 0.32 cm and gage length of 0.76 cm were machined from the plate materials. Most tests are being performed in conventional uniaxial lever arm constant load creep frames using resistance heating furnaces and shoulder-mounted extensometers at Metcut and GRC. However, two tests were run in specialized creep testing machines at GRC, which had

the specimens sealed within environmental chambers containing inert helium gas of 99.999 percent purity held slightly above atmospheric pressure. All creep tests were performed according to ASTM E139.

Tensile Tests.—Tensile test specimens were machined by Metcut having a gage diameter of about 0.40 cm and gage length of about 2.3 cm. Tensile tests were performed at Metcut and GRC in uniaxial test machines employing a resistance heating furnace and axial extensometer. The tests were performed according to ASTM E21, using an initial test segment with strain increased at a uniform rate of 0.2 percent per min, followed by a segment with displacement increased at a uniform rate of 5 mm/min.

Results and Discussion

Material and Microstructures

The actual chemistries in weight percent of all tested alloys are listed in table 1. Typical grain microstructures in optical images of etched metallographic sections of impeller materials are shown in figures 1 and 2. Grain width was approximated using grain linear intercept distance according to ASTM E112. LSHR had a fine, uniform grain microstructure, with an average linear intercept distance of about 29 μm , equivalent to a grain size of 7.0. Conventionally cast Mar-M247LC had more irregular, very coarse grains of near 700 μm width and near 800 to 12000 μm length, with grains often longer in the direction of primary dendrite growth. However, Microcast Mar-M247LC had a more uniform grain microstructure, with smaller grains of about 96 μm width (grain size = 3.5). IN792 had intermediate grain uniformity and size compared to the two versions of Mar-M247LC, with grain about 320 μm in width (grain size = 0). All the impeller alloys had microstructures predominated by 55 to 70 percent γ' precipitates in a γ matrix. MC and M_{23}C_6 carbides were also present. LSHR microstructure was predominated by about 55 vol% γ' precipitates in a γ matrix, but also contained minor MC and M_{23}C_6 carbides, M_3B_2 borides, and very fine oxides. Cooling γ' precipitate size was uniformly about 0.2 μm . Mar-M247LC and IN792 microstructure was predominated by about 65 to 70 vol% γ' precipitates in a γ matrix, with minor MC carbides. γ' precipitate sizes varied widely in these cast alloys, between about 0.4 and 3.0 μm , due to dendritic growth within grains.

Typical microstructures for plate materials are shown in figures 3 to 4. Hastelloy X, Inconel 617, Inconel 740, and Nimonic 263 had comparable grain sizes, but MA956 had much coarser grains. Hastelloy X and Inconel 617 had fairly uniform grain structures with mean grain sizes of about 69 and 75 μm (grain sizes of 4.4 and 4.2), respectively. They both were predominantly made up of γ phase, with minor contents of carbides. Inconel 617 also had about 2 vol% of γ' precipitates. However, these precipitates were very large at 1 to 10 μm diameter, and would not be expected to provide significant strengthening. Inconel 740 and Nimonic 263 had similar grain sizes of about 69 and 62 μm (grain sizes of 4.4 and 4.7), respectively. They both were predominantly made up of γ phase strengthened by about 20 to 25 vol% γ' precipitates, along with minor contents of carbides. The γ' precipitates were smaller in Inconel 740 than for Nimonic 263. Incoloy MA956 had a much coarser grain structure than the other duct alloys, with grains of flattened aspect ratio in the plane of the plate. Grains were typically 100 to 200 μm thick, but 300 to 1500 μm wide in the plane of the plate. This microstructure was predominantly made up of BCC ferrite phase, with minor contents of fine carbides and $\text{Y}_2\text{O}_3 - \text{Al}_2\text{O}_3$ dispersion strengthening particles. These chemistries and microstructures were typical of those reported in supplier references (refs. 3 to 12).

Mechanical Properties of Impeller Materials

Tensile Response.—Yield strengths at 0.2 percent offset, ultimate strengths, percent elongation after failure, and percent reduction in area after failure are compared as functions of temperature in table 3 and figure 5. LSHR had higher strength than Mar-M247LC at 978 K, but comparable strengths at 1090 and 1200 K. This could be related in part to the finer grain size of LSHR compared to both conventionally

cast and Microcast Mar-M247LC. Decreasing grain size has often been demonstrated to strongly improve strength in many superalloys (ref. 14) as well as other materials. However, the chemistries and precipitate contents of the two alloys would also influence their strengths. Microcast Mar-M247 had nearly identical strengths to conventionally cast Mar-M24LC at 1090 and 1200 K, even though the finer grain size of Microcast material would be expected to encourage higher strengths. IN792 had consistently lower strengths than both forms of Mar-M247LC and LSHR.

Ductility as indicated by elongation and reduction in area after failure is also compared as functions of temperature in table 3 and figure 5. LSHR had higher ductility than Mar-M247LC at 978 °C, but lower ductility at 1090 and 1200 K. Microcast Mar-M247 had lower ductility than conventionally cast Mar-M247LC at 1090 and 1200 K even though the strengths were comparable. IN792 had similar ductility to conventionally cast Mar-M247LC.

Creep Response.—Creep tests of impeller materials were designed to first screen the materials at temperatures of 978, 1090, and 1200 K. Subsequent tests were designed to ultimately determine allowable creep stresses for each material and temperature that would give 1 percent creep in 10 years of service, a goal then projected for JIMO applications. This service goal represented a target strain rate of 0.1 percent per year. Therefore, tests were performed to determine the allowable stress that would produce this strain rate at each of the test temperatures. Test conditions and results-to-date are listed for Mar-M247LC and LSHR in table 4. Initial tests of the third impeller material, IN792, are also included.

Tests to estimate the effects of air versus inert environments on creep resistance were initiated early on, using conventionally cast Mar-M247LC. The results of single tests in air at one atmosphere pressure and in helium slightly above one atmosphere at 1089 and 1200 K are compared in figure 6. Creep life in helium was lower than that for air in tests at 1089 K, but higher in tests at 1200 K. The differences were small at only 2 to 4×, which is near the normal scatter expected in creep response. More tests are needed for confirmation, but this appears to show relatively modest differences in life to 0.2 percent creep due to changing environment. A previous study that compared creep for superalloys in helium and air environments (ref. 3) also found only modest differences. However, other creep testing on LSHR has conclusively shown that creep loading in air encourages cracks to initiate at oxidized surfaces, causing failure (ref. 5). Therefore, LSHR and Mar-M247LC specimens tested to higher creep strains in air could initiate similar surface cracks at surface oxidation, giving accelerated creep response compared to specimens tested in helium. This could produce shorter creep lives in air than in helium. Eventually, creep tests in helium and air need to be continued to rupture at higher strains, in order to assess this issue.

Typical comparisons of time to 0.2 percent creep of LSHR and Mar-M247LC for temperatures of 977, 1089, and 1200 K are shown in figure 7. LSHR has slightly higher creep life at 977 K, but Mar-M247LC is superior at 1089 and 1200 K. This could be related in part to the much coarser grain size in Mar-M247LC compared to LSHR. The conventionally cast Mar-M247LC had a larger typical grain size than LSHR, as shown in figure 1. Increasing grain size has often been demonstrated to strongly improve superalloy creep resistance in these alloys (ref. 6). However, Mar-M247LC also has a different chemistry containing more aluminum and titanium to produce a content of γ' precipitates near 70 percent, compared to that of LSHR containing about 55 to 60 percent γ' . Mar-M247LC also has higher levels of the refractory elements tungsten, tantalum, niobium, and hafnium than does LSHR, which can all improve creep resistance of superalloys (ref. 4).

In order to examine the effects of only grain size on creep resistance, specimens from a bar of Mar-M247LC cast using the Microcast process were obtained, containing finer grains compared to conventionally cast material, figure 1. Limited comparison tests indicate the Microcast specimens had 2 to 10× lower creep life than conventionally cast Mar-M247LC, figure 8. The initial tests of IN792 are also included for comparison, as its content of γ' and microstructure were similar to Mar-M247LC. IN792 material was cast using a proprietary Grainex process that also produced a finer grain size than conventionally cast Mar-M247LC. It also had lower creep resistance, comparable to Microcast Mar-M247LC. This illustrated the strong effect of increasing grain size on creep resistance at high

temperatures, and should be kept in mind when selecting processing paths for both impeller and duct alloys. This grain size difference more strongly affected creep resistance than strength for this alloy.

Creep results of all tests were used to generate conventional Larson-Miller curves of stress versus Larson-Miller parameter (*LMP*) using temperature (*T*) and time (*t*) in the equation (ref. 15):

$$LMP = (T)(20 + \log t)/1000$$

This parameter has a direct dependence with temperature, but a weaker logarithmic dependence of time. The resulting plot is shown in figure 9. The *LMP* curves confirm consistently higher comparative response for LSHR at combinations of high stress and low temperatures, but higher response for Mar-M247LC at combinations of low stress and high temperatures. Simple regression equations are included for estimating creep response at intermediate conditions. However, it is not advisable to use these equations to estimate creep response at times greater than 10 times over that of the input data, which extended to 7,295 h.

Creep strain rate to 0.2 percent is shown versus stress in figures 10 to 11. These plots allowed initial estimation of allowable stresses for achieving the target strain rate of 0.1 percent per yr. for each material. At 978 K, a stress of about 350 MPa was estimated for both LSHR and Mar-M247LC. However, at higher temperature the superior creep resistance of Mar-M247LC over LSHR was clearly reflected in the estimated stresses. A stress of 100 MPa was estimated for Mar-M247LC at 1090 K, while no stress could be estimated for LSHR. At 1200 K, a stress could no longer be clearly estimated for either material, although Mar-M247LC again had much better creep resistance. Additional creep tests and analyses are necessary, but a preliminary creep analysis using current test results indicates quite good potential for an impeller fabricated of Mar-M247LC to meet Brayton cycle requirements, for maximum temperatures below 1200 K (ref. 16).

Mechanical Properties of Duct Materials

Tensile Response.—Comparative duplicate tensile tests were performed at 1090 and 1200 K for most of the duct materials. Incoloy MA956 was not tensile tested due to an insufficient material supply. Average yield strengths at 0.2 percent offset and ultimate strengths are compared as functions of temperature in figure 12. Inconel 740 had highest strength among the duct alloys tested. Hastelloy X had lowest strength at 1090 K, while Nimonic 263 had lowest strength at 1200 K. As a group, the precipitation strengthened alloys Inconel 740 and Nimonic 263 had significantly higher strength than the solid solution alloys Hastelloy X and Inconel 617 at 1090 K. At 1200 K the precipitation strengthening improvement over the predominantly solid solution alloys was still evident for Inconel 740, but not for Nimonic 263. Now both these alloys would be expected to have comparable amounts of γ' precipitates at 1200 K, based on their similar compositions including the amounts of Al + Ti which stabilize γ' . However, Nimonic 263 appeared to have significantly larger precipitates even before testing at 1200 K, and this larger precipitate size may be less effective in strengthening at high temperatures.

Ductility as indicated by elongation and reduction in area after failure is also compared as functions of temperature in figure 12. Hastelloy X had the highest ductility among the duct alloys at 1090 K, while Inconel 740 had the lowest ductility. As a group, the predominantly solid solution strengthened alloys Hastelloy X and Inconel 617 had superior ductilities to the precipitation strengthened alloys Inconel 740 and Nimonic 263 at 1090 K. At 1200 K, all duct alloys had very good ductilities exceeding 50 percent reduction in area, with no consistent trends among the alloys.

Additional tensile tests were performed on Inconel 617 to compare tensile properties in the plate longitudinal and width directions. Averaged yield and ultimate strengths are compared with associated elongations and reductions in area in figure 13. Strengths and ductilities were quite comparable in the two plate directions, for tests performed at 300, 1090, and 1200 K.

Creep Response.—Vendor literature contained appreciable information on the creep resistance of these materials for temperatures near 977 K, but had little data at higher temperatures. Therefore, creep

tests of duct/heat exchanger materials were designed to screen the materials at temperatures of 1090 and 1200 K. Subsequent tests designed to determine allowable stresses for each alloy based on service goals have not yet been started, due to the variety of duct and heat exchanger applications possible here, as well as recent changes in program goals. Current test conditions and results are listed for Hastelloy X, Inconel 617, Inconel 740, Nimonic 263, and Incoloy MA956 in table 3.

Typical comparisons of time to 0.1, 0.2, and 0.3 percent creep of these materials at 1089 K are shown in figure 14, for duplicate tests at a stress of 103 MPa. Of the solid solution strengthened superalloys, Inconel 617 had about 10x better creep resistance than Hastelloy X. However, the γ' precipitate strengthened superalloys Inconel 740 and Nimonic 263 had about 20x improved creep resistance over Inconel 617. These results indicate Inconel 617, Inconel 740, and Nimonic 263 had good creep resistance for potential applications at 1089 K, while Hastelloy X would be at a definite disadvantage. Additional testing would be necessary to determine allowable stresses for each alloy.

Typical comparisons of time to 0.1 and 0.2 percent creep of these materials at 1200 K are shown in figure 15, for single tests at a very low stress of 14 MPa. The materials had much lower creep resistance at this temperature. Of the solid solution strengthened superalloys, Inconel 617 had 2 to 3 times better creep resistance than Hastelloy X. However, the γ' precipitate strengthened superalloys Inconel 740 and Nimonic 263 had mixed response. Nimonic 263 had comparable creep resistance to Inconel 617, while Inconel 740 had lower creep resistance than Hastelloy X as well as Inconel 617. This could be related to the potential for precipitation of harmful phases in Inconel 740 and Nimonic 263 at this temperature (ref. 12). Incoloy MA956 had much better creep resistance than the other materials at 1200 K, but does have many component processing issues. It would therefore be expected that Inconel 617 and Nimonic 263 have potential for 1200 K applications, though at very low stresses. Incoloy MA956 could have potential for application for higher stresses, but would require an extensive process development program in order to form and join duct components from this alloy.

Several creep tests were performed at 1200 K to compare the relative creep resistance of Hastelloy X and Inconel 617 in the plate longitudinal and width directions. Specimens in the plate longitudinal direction had superior response for both alloys, as shown in figure 16. While the differences were only 2 to 3x, this direction dependence could be an important consideration in duct design, where internal pressure-induced stresses for tubes rolled from flat plates are often highest in the hoop direction.

Impeller and Duct Material Selection

Impeller material.—For applications having maximum temperatures near 978 K, current results indicate LSHR would appear to be the preferable impeller material. It has higher strength than Mar-M247LC and IN792, and creep resistance as good as Mar-M247LC. Other work currently being prepared for publication indicates LSHR also has far superior high cycle fatigue resistance to Mar-M247LC in tests at 978 and 1090 K. For applications having maximum temperatures of 1090 K and higher, conventionally cast Mar-M247LC would appear to be the material of choice. It had far superior creep response to LSHR and IN792, with roughly comparable tensile strength at these temperatures. This was related in part to the coarse grain size of the conventionally cast Mar-M247LC bars. Indeed, the differences in response between Mar-M247LC and IN792 may be largely due to their different casting processes. Inspection of table 1 indicates that Mar-M247LC and IN792 have very similar compositions with respect to total content of γ' stabilizing elements (Al+Ti+Ta+Nb+Hf), although hafnium is absent in IN792. Yet IN792 was cast as an actual impeller for an auxiliary power unit using a common fine grain casting process, while most Mar-M247LC were conventionally cast as simple bars. The IN792 properties may therefore reflect those to be expected in Mar-M247LC, when the latter alloy is cast into impellers using typical production casting practices (ref. 17).

Duct Materials.—For applications having maximum temperatures of 978 to 1089 K, current results indicate Inconel 617 would be the solid solution strengthened material of choice over Hastelloy X, due to superior creep resistance. This alloy would be relatively easy to fabricate into duct components. The precipitation strengthened alloys Inconel 740 and Nimonic 263 offer further improvements in creep

resistance. However, significant additional process development efforts would be necessary to shape, join, and heat treat duct components for these alloys. For applications having maximum temperatures of 1200 K, none of the tested duct alloys looked overly promising. Inconel 617 could be the preferable selection, albeit at low creep stresses. Inconel 740 and Nimonic 263 offered no evident improvements in creep resistance, and would again have the processing development issues and also phase stability questions. Incoloy MA956 might offer improvements in creep resistance, but would have extensive processing issues to be addressed.

Summary and Conclusions

Two cast superalloys, Mar-M247LC and IN792, and a NASA powder metallurgy superalloy, LSHR, were screened to compare their respective capabilities for impeller applications. Several wrought superalloys including Hastelloy X, Inconel 617, Inconel 740, Nimonic 263, and Incoloy MA956 were also screened to compare their capabilities for duct applications. Conventional tensile and creep tests were performed at temperatures up to 1200 K on specimens extracted from the materials. Initial microstructure evaluations were also undertaken. The results can be summarized as follows:

(1) Impeller materials: LSHR had higher strength than Mar-M247LC and IN792 at 978 K, but comparable strengths at 1090 and 1200 K. LSHR had comparable creep resistance to Mar-M247LC at 978 K. At higher temperatures, conventionally cast Mar-M247LC had superior creep resistance. Initial estimates suggest a target strain rate of 0.1 percent per year for Mar-M247 could be achieved at 100 MPa and 1090 K or 350 MPa and 978 K.

(2) Duct/heat exchanger materials: The precipitate strengthened superalloys Inconel 740 and Nimonic 263 had improved creep response over solid solution strengthened superalloys Inconel 617 and Hastelloy X at temperatures to 1090 K. At temperatures near 1200 K, all these alloys had low creep stress bearing capabilities. Mechanically alloyed Incoloy MA956 had improved creep resistance at this temperature.

It can be concluded from this evaluation that LSHR should be further evaluated for impeller applications with maximum temperatures near 978 K. Mar-M247LC and IN792 should be further evaluated for impeller applications requiring higher temperatures. The solid solution strengthened superalloy Inconel 617 should be further evaluated for duct applications at maximum temperatures up to 1089 K. A precipitation hardened alloy such as Nimonic 263 should also be further studied for duct applications. For both impeller and duct materials, the material processing and fabrication procedures necessary to produce these components should also be considered and screened, in order to assess material potentials and properties as real components.

References

1. L.S. Mason, "A Power Conversion Concept for the Jupiter Icy Moons Orbiter," *Journal of Propulsion and Power*, vol. 20, no. 5, Sept. 2005, pp. 902–910.
2. M.J. Barrett, "Expectations of Closed-Brayton-Cycle Heat Exchangers in Nuclear Space Power Systems," *Journal of Propulsion and Power*, vol. 21, no. 1, January 2005, pp. 152–157.
3. R.L. Ammon, L.R. Eisenstatt, and G.O. Yatsko, "Creep Rupture Behavior of Selected Turbine Materials in Air, Ultra-High Purity Helium, and Simulated Closed Cycle Brayton Helium Working Fluids," *Journal of Engineering for Power*, vol. 103, April 1981, pp. 331–337.
4. K. Harris, G.L. Erickson, and R.E. Schwer, "Development of a High Creep Strength, High Ductility, Cast Superalloy for Integral Turbine Wheels," 1982 AIME Annual Meeting, Feb. 1982.
5. C.T. Sims, N.S. Stoloff, and W.C. Hagel, *Superalloys II*, John Wiley & Sons, New York, NY, 1987, pp. 583–585.

6. T.P. Gabb, J. Gayda, J. Telesman, and P.T. Kantzos, "Thermal and Mechanical Property Characterization of the Advanced Disk Alloy LSHR," NASA/TM—2005-213645, Washington, D.C., June 2005.
7. "Hastelloy X Alloy," technical publication by Haynes International, Inc., 1997.
8. "Inconel alloy HX," technical publication by Special Metals Corp., 2003.
9. "Inconel alloy 617," technical publication by Special Metals Corp., 2005.
10. "Incoloy alloy MA956," technical publication by Special Metals Corp., 2003.
11. "Inconel alloy 740," technical publication by Special Metals Corp., 2004.
12. G. Smith, L. Shoemaker, "Advanced Nickel Alloys For Coal-Fired Boiler Tubing," *Advanced Materials and Processes*, July 2004, pp. 23–26.
13. "Nimonic alloy 263," technical publication by Special Metals Corp., 2003.
14. C.T. Sims, N.S. Stoloff, and W.C. Hagel, *Superalloys II*, John Wiley & Sons, New York, NY, 1987, p. 477.
15. F.R. Larson and J. Miller, *Trans. ASME*, vol. 74, 1952, pp. 765–766.
16. J. Gayda, and T.P. Gabb, "Two-Dimensional Viscoelastic Stress Analysis of a Prototypical JIMO Turbine Wheel," NASA/TM—2005-213650, Washington, D.C., June, 2005.
17. I.R. Delgado, G.R. Halford, B.M. Steinetz, and C.M. Rimnac, "Strain-Life Assessment of Grainex Mar-M247 for NASA's Turbine Seal Test Facility," NASA/TM—2004-212985 (ARL-TR-3178), National Aeronautics and Space Administration, Washington, D.C., April 2004.

TABLE 1.—MEASURED CHEMISTRIES OF IMPELLER AND DUCT SUPERALLOYS

Alloy, wt%	Al	B	C	Co	Cr	Cu	Fe	Hf	Mh	Mo	Ni	Nb	O	Si	Ta	Ti	V	W	Y	Zr
NASA LSHR	3.46	0.028	0.029	20.7	12.52	-----	0.07	-----	-----	2.73	Bal.	1.45	-----	0.03	1.6	3.5	-----	4.33	-----	0.049
Conv. Cast Mar-M247LC	5.6	0.015	0.09	9.4	8.3	-----	-----	1.4	0.02	0.5	Bal.	-----	-----	0.01	3.2	0.7	-----	9.5	-----	0.011
Microcast Mar-M247LC	5.52	0.002	0.0855	9.31	8.52	-----	0.04	1.46	-----	0.51	Bal.	-----	-----	0.05	3.15	0.75	-----	9.47	-----	0.011
IN792	3.45	0.0015	0.08385	8.95	12.635	-----	0.01	0.02	-----	1.83	Bal.	-----	-----	0.03	3.975	3.835	-----	4.08	-----	0.015
Hastelloy X	0.19	-----	0.0855	1.01	21.435	0.24	19.485	-----	0.525	8.5	Bal.	0.115	-----	0.31	0.008	0.02	0.025	0.455	-----	-----
Incone1 617	0.985	-----	0.0945	11.64	22.65	0.05	0.905	-----	0.04	9.45	Bal.	0.12	-----	0.155	0.008	0.36	0.0055	0.035	-----	-----
Incone I 740	0.93	-----	0.031	19.945	24.24	0.04	0.445	-----	0.25	0.51	Bal.	1.96	-----	0.525	-----	1.71	-----	0.01	-----	0.011
Nimonic 263	0.45	-----	0.061	19.3	20.45	0.02	0.38	-----	0.33	5.8	Bal.	0.05	-----	0.125	0.0065	2.19	-----	0.01	-----	-----
Incoloy MA956	4.555	-----	0.01675	-----	19.7	0.01	Bal.	-----	0.09	0.01	0.13	0.005	0.2035	0.08	-----	0.365	0.025	0.01	0.29	-----

TABLE 2.—TENSILE TEST RESULTS FOR IMPELLER SUPERALLOYS

		Temperature, °F	Temperature, K	0.2% yield, ksi	Yield, MPa	Ultimate tensile strength, ksi	Ultimate tensile strength, MPa	Elongation, %	Reduction in area, %
LSHR	Tensile	1300	978	136.9	944	184.9	1275	24.0	32.6
LSHR	Tensile	1300	978	155.6	1073	200.1	1380	10.4	11.7
Mar-M247LC	Tensile	1300	978	111.3	767	151.6	1045	12.9	23.0
Mar-M247LC	Tensile	1300	978	111.1	766	145.7	1005	12.1	19.1
LSHR	Tensile	1500	1089	119.3	823	143.6	990	13.8	20.6
LSHR	Tensile	1500	1089	133.9	923	157.0	1083	5.6	10.6
Mar-M247LC (Conv.)	Tensile	1500	1089	121.4	837	147.2	1015	9.3	23.0
Mar-M247LC (Conv.)	Tensile	1500	1089	120.2	829	147.9	1020	11.9	30.7
Mar-M247LC (Micro.)	Tensile	1500	1089	117.1	807	147.8	1019	5.4	10.2
IN792	Tensile	1500	1089	104.5	721	135.4	934	9.0	21.5
LSHR	Tensile	1700	1200	71.8	495	94.8	654	10.4	15.6
LSHR	Tensile	1700	1200	76.9	530	95.4	658	5.6	8.7
Mar-M247LC (Conv.)	Tensile	1700	1200	73.3	505	106.2	732	9.8	15.6
Mar-M247LC (Conv.)	Tensile	1700	1200	73.2	505	106.7	736	12.1	20.8
Mar-M247LC (Micro.)	Tensile	1700	1200	75.5	521	107.9	744	4.9	7.2
IN792	Tensile	1700	1200	61.6	425	86.7	598	18.5	25.1

TABLE 3.—CREEP TEST RESULTS FOR IMPELLER SUPERALLOYS

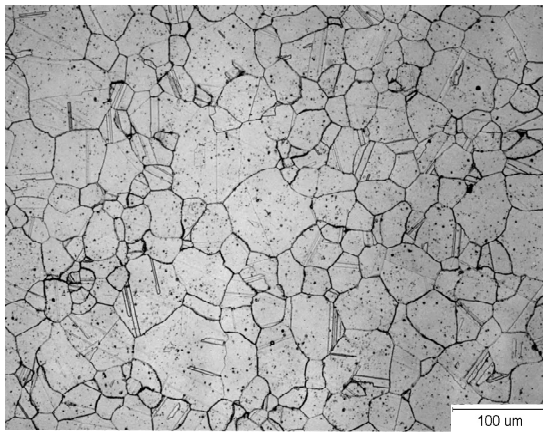
Alloy	Process	Temperature, °F	Temperature, K	Stress, ksi	Stress, MPa	0.1% creep life, h	0.2% creep life, h	0.3% creep life, h	Rupture life, h	Elongation, %	Reduction in area, %	Notes
LSHR	PM Disk	1200	922	90	621	90.9	3769.4	---	-----	---	---	
LSHR	PM Disk	1300	978	100	690	115.0	174.0	---	-----	---	---	
LSHR	PM Disk	1300	978	100	690	149.0	254.0	---	-----	---	---	
LSHR	PM Disk	1300	978	80	552	1877.0	3082.0	---	-----	---	---	
LSHR	PM Disk	1500	1089	45	310	61.0	281.0	603	1068.7	5.8	6.5	
LSHR	PM Disk	1500	1089	30	207	414.0	1098.0	---	-----	---	---	
LSHR	PM Disk	1500	1089	15	103	1805.0	3356.0	---	-----	---	---	
LSHR	PM Disk	1500	1089	3	21	478.0	3888.0	---	-----	---	---	
LSHR	PM Disk	1500	1089	25	172	6.8	80.0	---	-----	---	---	
LSHR	PM Disk	1700	1200	20	138	5.7	13.6	---	121.7	8.8	10	
LSHR	PM Disk	1700	1200	10	69	9.9	24.7	40	664.9	26.9	28.4	
LSHR	PM Disk	1700	1200	5	34	30.5	86.0	---	3109.6	83	56.9	
MM247LC	ConvCastBar	1300	978	100	690	30.0	104.0	---	-----	---	---	
MM247LC	ConvCastBar	1300	978	100	690	18.6	55.0	---	-----	---	---	
MM247LC	ConvCastBar	1300	978	80	552	1424.0	3416.0	---	-----	---	---	
MM247LC	ConvCastBar	1500	1089	45	310	515.0	1014.0	---	-----	---	---	
MM247LC	ConvCastBar	1500	1089	30	207	1296.0	7295.0	---	-----	---	---	
MM247LC	ConvCastBar	1500	1089	30	207	502.5	1952.0	---	-----	---	---	Helium env.
MM247LC	ConvCastBar	1700	1200	30	207	29.0	74.0	187	546.4	7.6	12.4	
MM247LC	ConvCastBar	1700	1200	20	138	837.0	1422.0	---	-----	---	---	
MM247LC	ConvCastBar	1700	1200	10	69	334.1	3454.1	---	-----	---	---	
MM247LC	ConvCastBar	1700	1200	10	69	2274.0	5891.0	---	-----	---	---	Helium env.
MM247LC	MicroCastBar	1300	978	80	552	634.7	---	---	-----	---	---	
MM247LC	MicroCastBar	1500	1089	45	310	48.7	188.0	---	-----	---	---	
IN792GX	Grainex Cast Impeller	1300	978	80	552	1153.8	---	---	-----	---	---	
IN792GX	Grainex Cast Impeller	1300	978	80	552	146.0	940.0	---	-----	---	---	
IN792GX	Grainex Cast Impeller	1500	1089	45	310	126.0	340.0	---	-----	---	---	
IN792GX	Grainex Cast Impeller	1500	1089	45	310	110.0	272.0	764	-----	---	---	

TABLE 4.—TENSILE TEST RESULTS FOR DUCT SUPERALLOYS

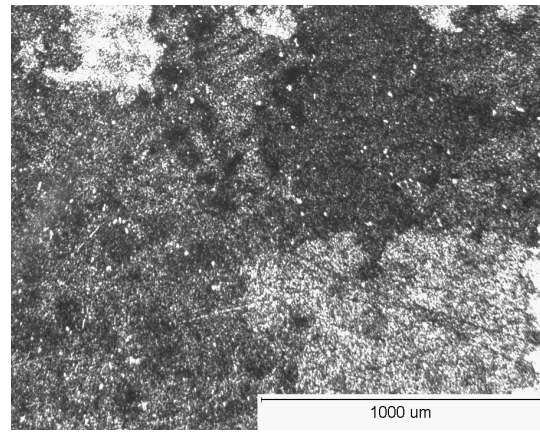
Alloy	Test	Orientation	Temperature, °F	Temperature, K	0.2% yield, ksi	Yield, MPa	Ultimate tensile strength, ksi	Ultimate tensile strength MPa	Elongation, %	Reduction in area, %
Inconel 617	Tensile	Longitudinal	75	297	70	483	123	848	47	58
Inconel 617	Tensile	Longitudinal	75	297	70	483	124	855	46	58
Inconel 617	Tensile	Width	75	297	66.5	459	122	841	49	59
Inconel 617	Tensile	Width	75	297	66.5	459	122	841	49	59
Hastelloy X	Tensile	Longitudinal	1500	1089	24.6	170	48	331	67	78
Hastelloy X	Tensile	Longitudinal	1500	1089	24.4	168	48.6	335	66	75
Inconel 617	Tensile	Longitudinal	1500	1089	40.6	280	57	393	45	55
Inconel 617	Tensile	Longitudinal	1500	1089	40.6	280	57	393	51	54
Inconel 617	Tensile	Width	1500	1089	41.7	288	56	386	50	56
Inconel 617	Tensile	Width	1500	1089	42.5	293	56.5	390	49	55
Inconel 740	Tensile	Longitudinal	1500	1089	73	503	90.5	624	8.5	18
Inconel 740	Tensile	Longitudinal	1500	1089	70	483	85.5	590	8	16
Nimonic 263	Tensile	Longitudinal	1500	1089	62	427	80	552	27	47
Nimonic 263	Tensile	Longitudinal	1500	1089	60	414	79	545	28	43
Hastelloy X	Tensile	Longitudinal	1700	1200	18.6	128	26.9	185	77	81
Hastelloy X	Tensile	Longitudinal	1700	1200	19.3	133	27.5	190	80	84
Inconel 617	Tensile	Longitudinal	1700	1200	21.4	148	31.1	214	54	59
Inconel 617	Tensile	Longitudinal	1700	1200	21.8	150	31.6	218	52	55
Inconel 617	Tensile	Width	1700	1200	22.9	158	31.2	215	49	53
Inconel 617	Tensile	Width	1700	1200	24.9	172	31.9	220	49	60
Inconel 740	Tensile	Longitudinal	1700	1200	29.1	201	35.8	247	47	86
Inconel 740	Tensile	Longitudinal	1700	1200	30.1	208	35.7	246	46	79
Nimonic 263	Tensile	Longitudinal	1700	1200	16.1	111	24.6	170	78	96
Nimonic 263	Tensile	Longitudinal	1700	1200	16.4	113	24.7	170	73	95

TABLE 5.—CREEP TEST RESULTS FOR DUCT SUPERALLOYS

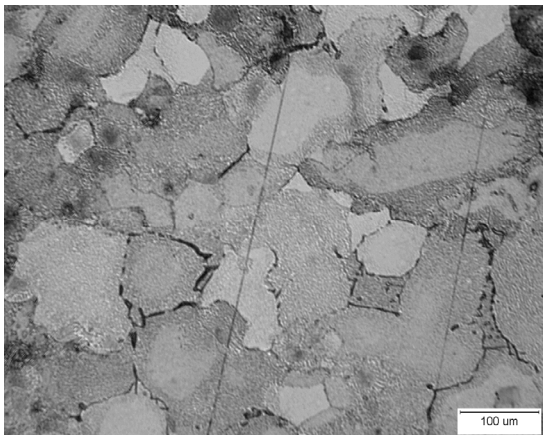
Alloy	Process	Temperature, °F	Temperature, K	Stress, ksi	Stress, MPa	0.1% creep life, h	0.2% creep life, h	0.3% creep life, h	Rupture life, h	Elongation, %	Reduction in area, %
Hastelloy X	Plate	1500	1089	15	103	0.5	0.8	1.8	97.3	64.6	76.1
Hastelloy X	Plate	1500	1089	15	103	0.4	0.7	1.7	-----	-----	-----
Hastelloy X	Plate	1700	1200	5	34	0.6	3.1	9.8	459.6	77.8	-----
Hastelloy X	Plate	1700	1200	2	14	107.0	314.0	-----	-----	-----	-----
Hastelloy X	Plate	1700	1200	2	14	48.0	254.0	941	-----	-----	-----
Inconel 617	Plate	1500	1089	15	103	1.5	8.3	19	-----	-----	-----
Inconel 617	Plate	1500	1089	15	103	1.8	10.9	-----	769.3	29.4	34.6
Inconel 617	Plate	1700	1200	5	34	157.0	480.0	785	2028.1	13.2	19.9
Inconel 617	Plate	1700	1200	2	14	216.0	1092.0	-----	-----	-----	-----
Inconel 617	Plate	1700	1200	2	14	58.0	361.0	1737	-----	-----	-----
Inconel 740	Plate	1500	1089	15	103	115.0	277.0	741	-----	-----	-----
Inconel 740	Plate	1500	1089	15	103	245.0	470.0	667	-----	-----	-----
Inconel 740	Plate	1700	1200	5	34	8.7	26.0	71	1563.6	40	51.3
Inconel 740	Plate	1700	1200	2	14	35.8	96.0	145	-----	-----	-----
Nimonic 263	Plate	1500	1089	15	103	193.0	355.0	474	-----	-----	-----
Nimonic 263	Plate	1500	1089	15	103	78.0	257.0	358	1978.8	20.3	19.4
Nimonic 263	Plate	1700	1200	5	34	0.9	2.4	-----	239.2	35.5	33.2
Nimonic 263	Plate	1700	1200	2	14	400.0	754.0	1042	-----	-----	-----
MA956	Plate	1700	1200	2	14	5995.0	-----	-----	-----	-----	-----



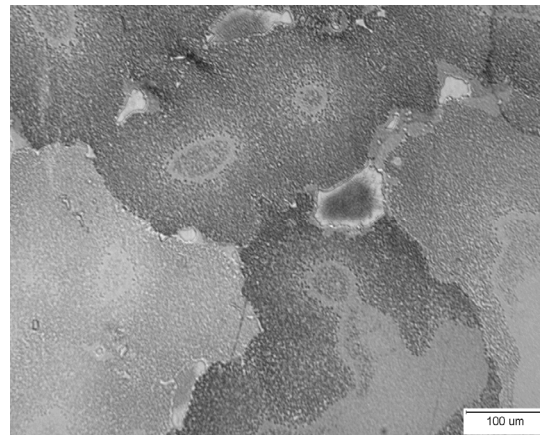
a) LSHR



b) Conventionally Cast Mar-M247LC

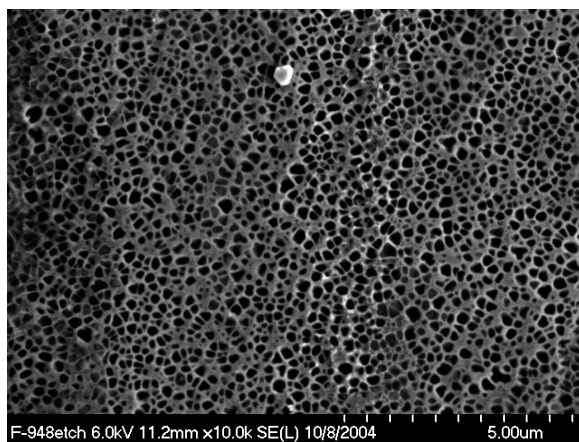


c) Microcast Mar-M247LC

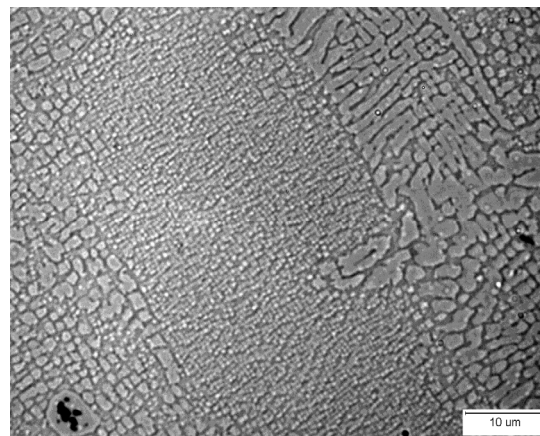


d) IN792

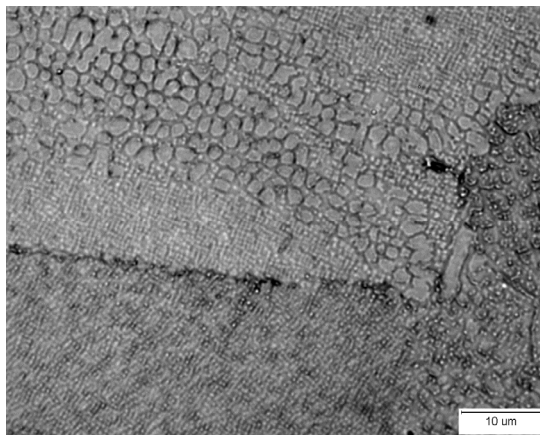
Figure 1.—Typical microstructures of impeller alloys: a) LSHR, b) conventionally cast Mar-M247LC, c) Microcast Mar-M247LC, d) IN792.



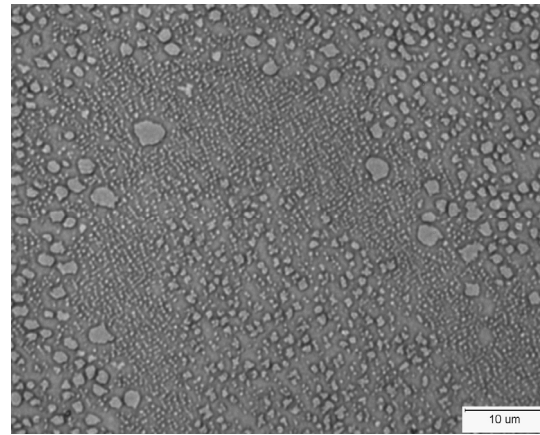
a) LSHR



b) Conventionally Cast Mar-M247LC

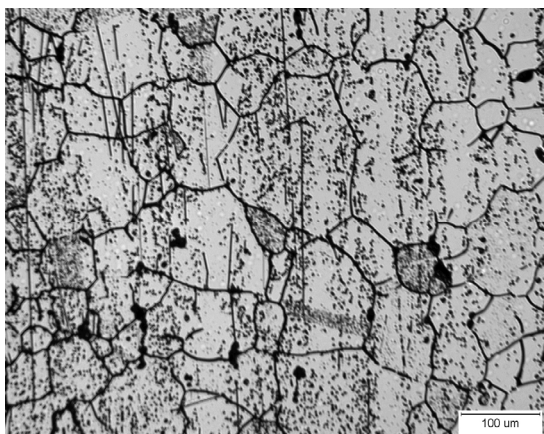


c) Microcast Mar-M247LC

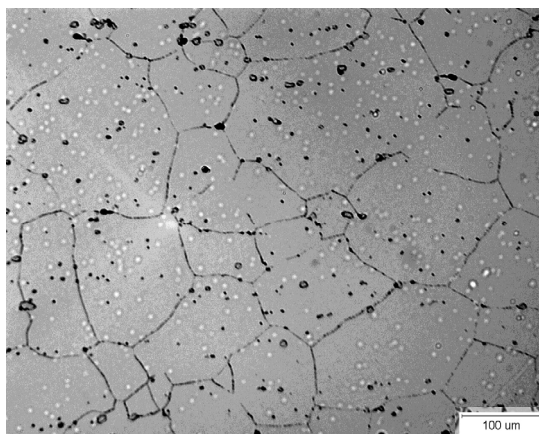


c) IN792

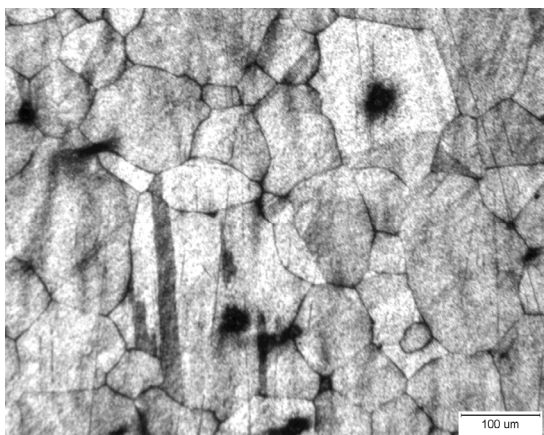
Figure 2.—Typical microstructures of impeller alloys: a) LSHR, b) conventionally cast Mar-M247LC, c) Microcast Mar-M247LC, d) IN792.



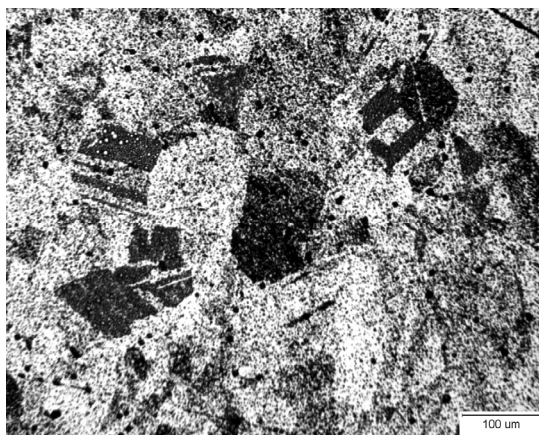
a) Hastelloy X



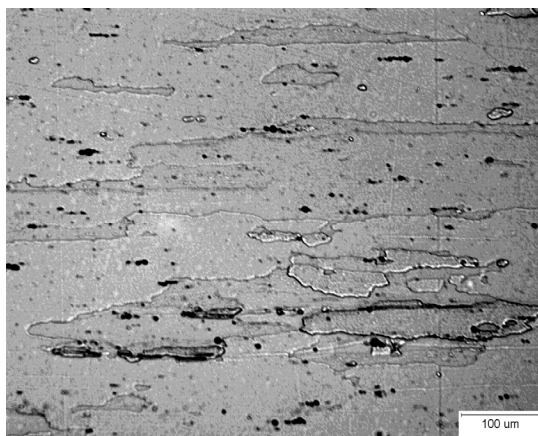
b) Inconel 617



c) Inconel 740

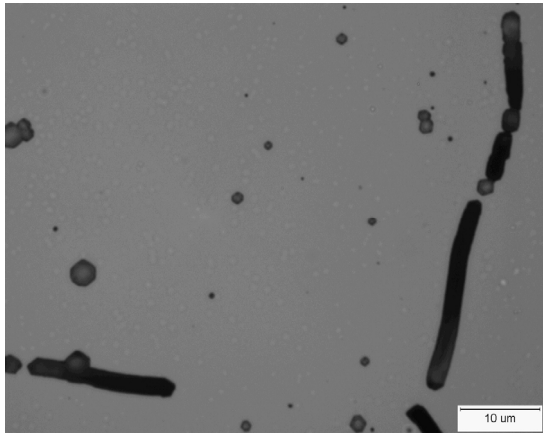


d) Nimonic 263

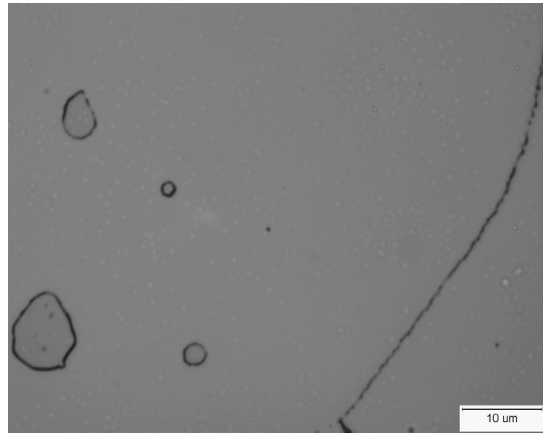


e) Incoloy MA956

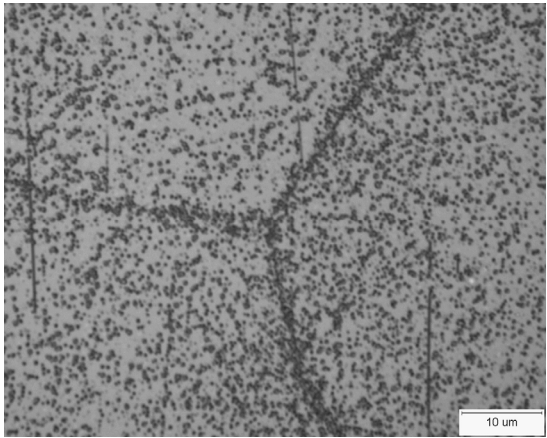
Figure 3.—Typical microstructures of duct superalloys: a) Hastelloy X, b) Inconel 617, c) Inconel 740, d) Nimonic 263, e) Incoloy MA 956.



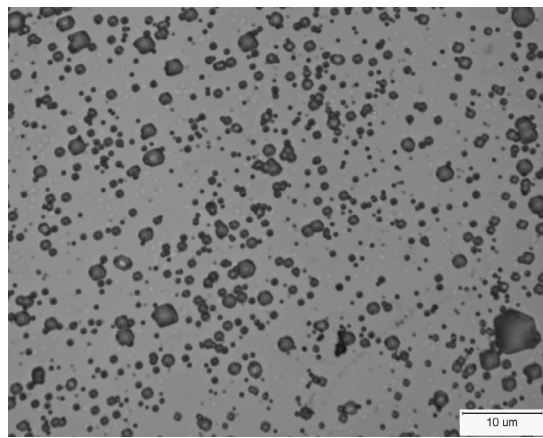
a) Hastelloy X



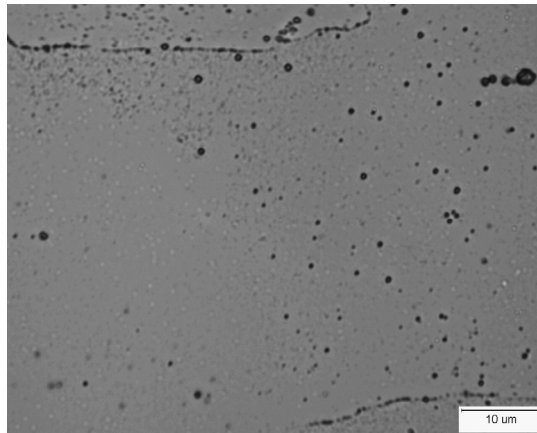
b) Inconel 617



c) Inconel 740



d) Nimonic 263



e) Incoloy MA956

Figure 4.—Typical microstructures of duct superalloys: a) Hastelloy X, b) Inconel 617, c) Inconel 740, d) Nimonic 263, e) Incoloy MA 956.

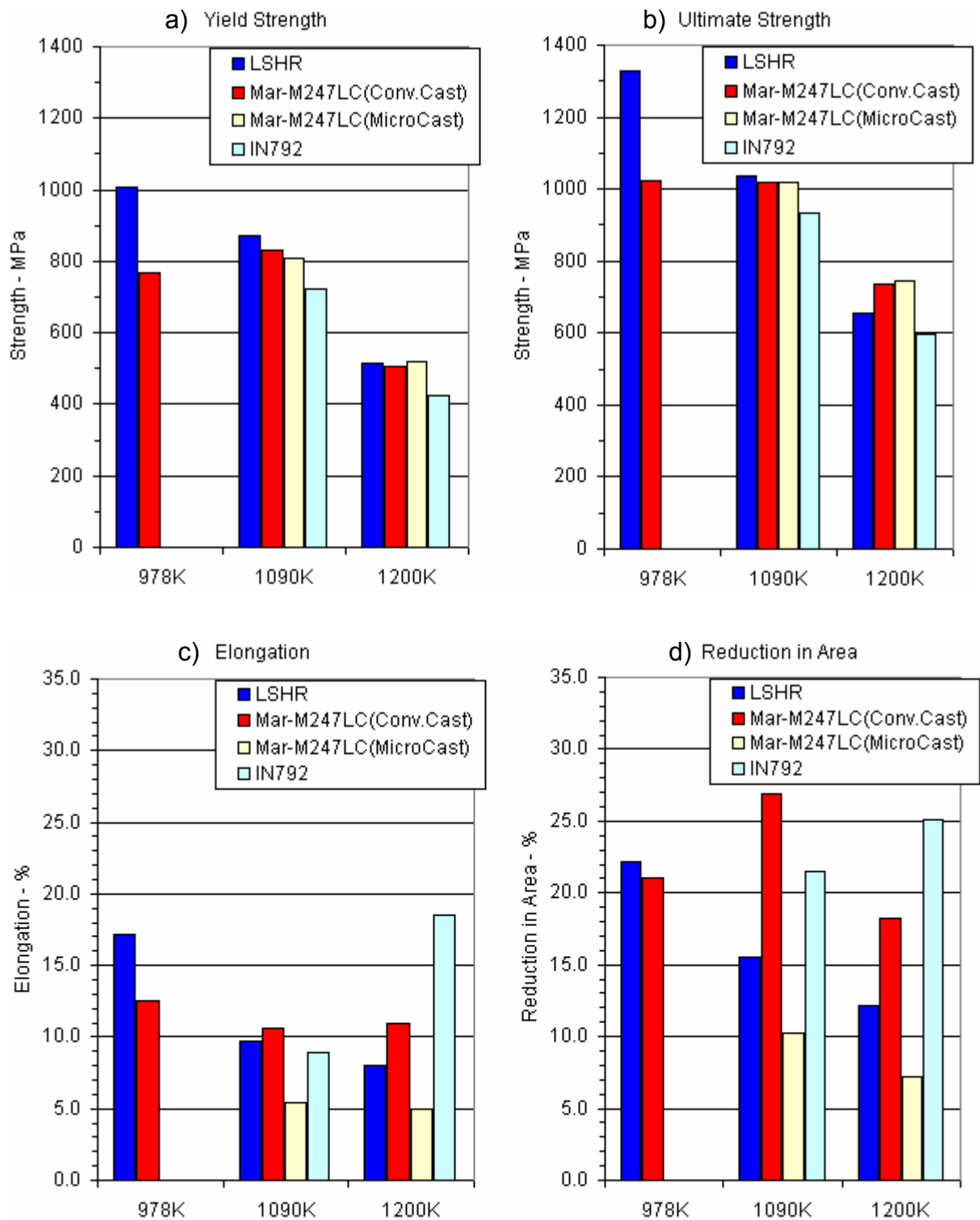


Figure 5.—Tensile response of impeller alloys: a) yield strength, b) ultimate strength, c) elongation, d) reduction in area.

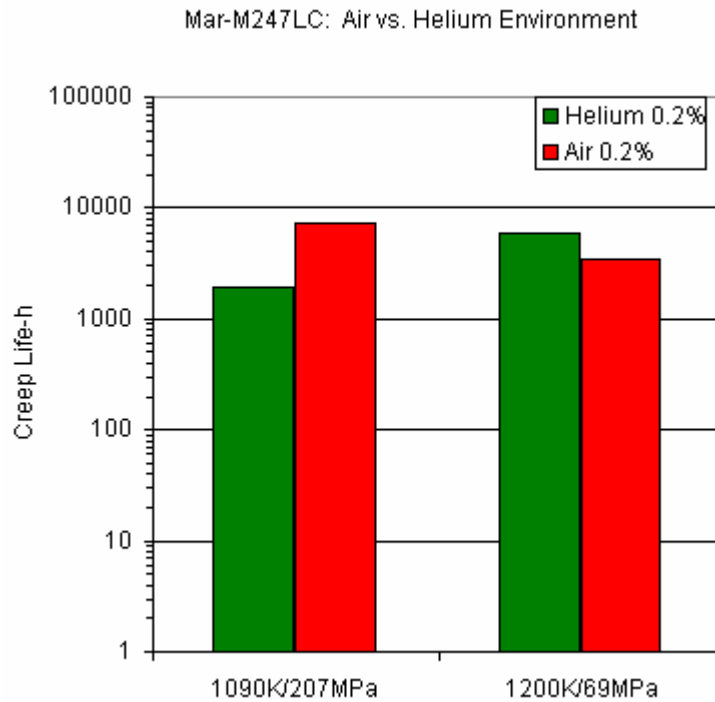


Figure 6.—Comparison of creep response of conventionally cast Mar-M247LC in helium and air.

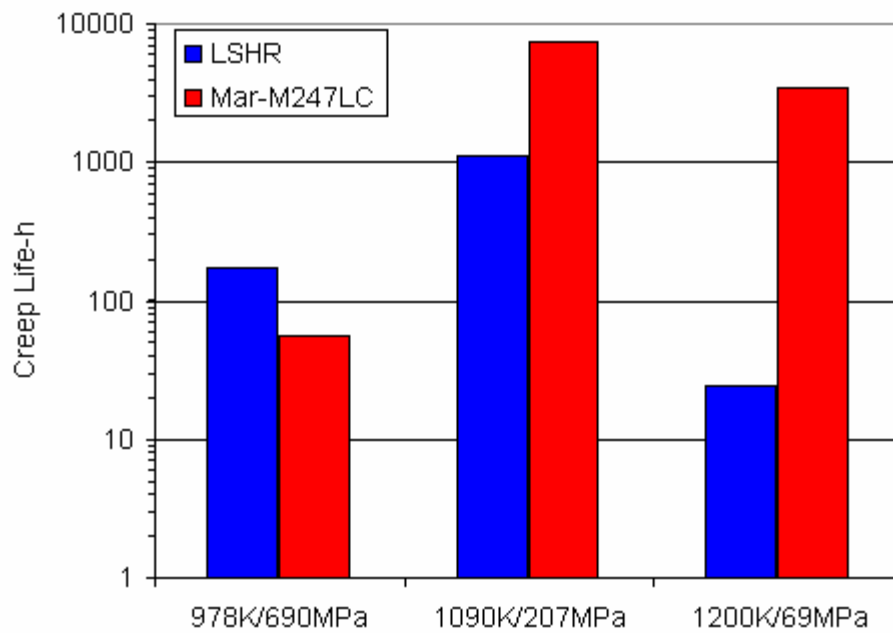


Figure 7.—Comparison of creep response of LSHR and conventionally cast Mar-M247LC.

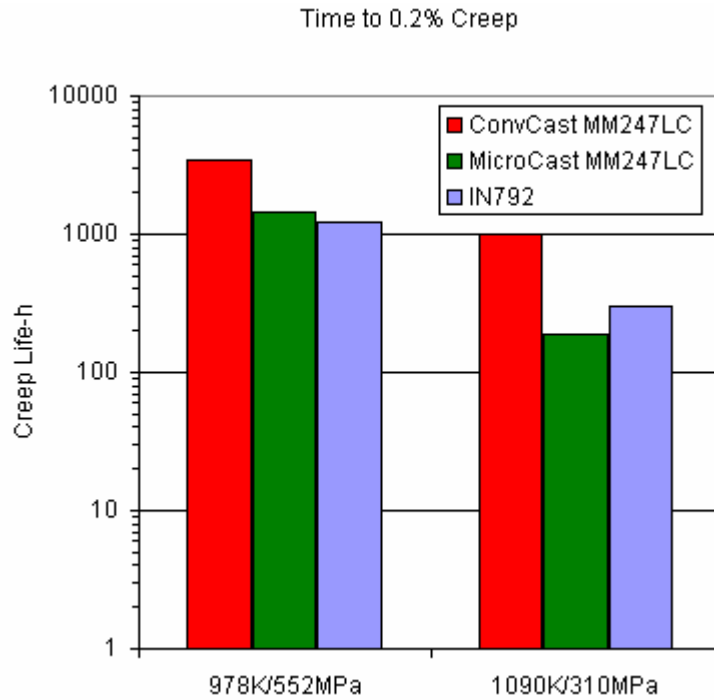


Figure 8.—Comparison of creep response of conventionally cast and Microcast® Mar-M247LC, along with IN792.

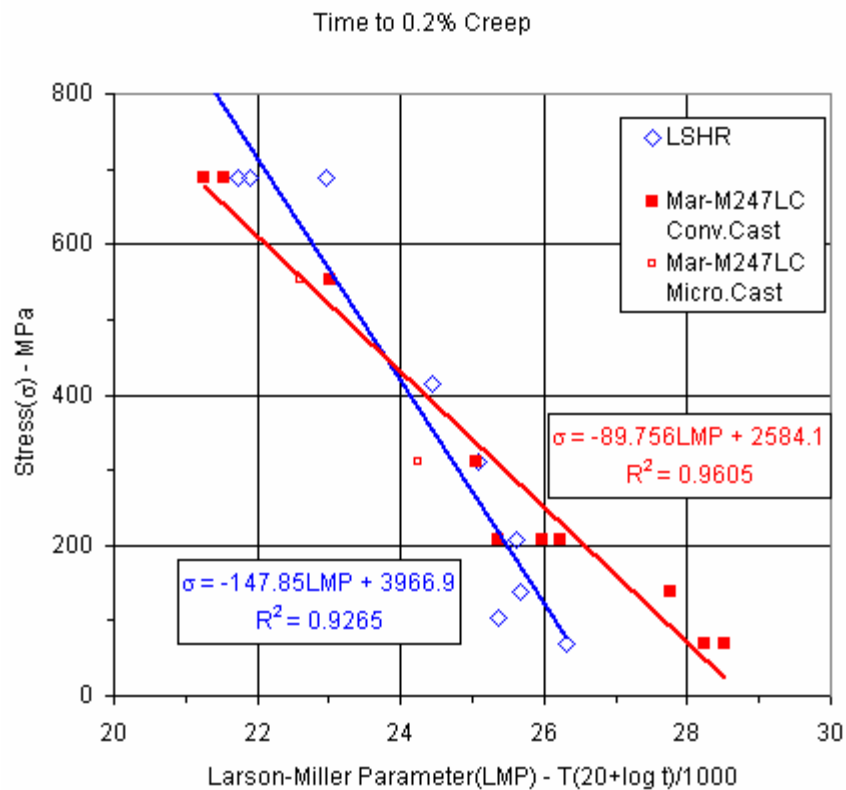


Figure 9.—Larson-Miller parameter comparison of creep response of LSHR and Mar-M247LC.

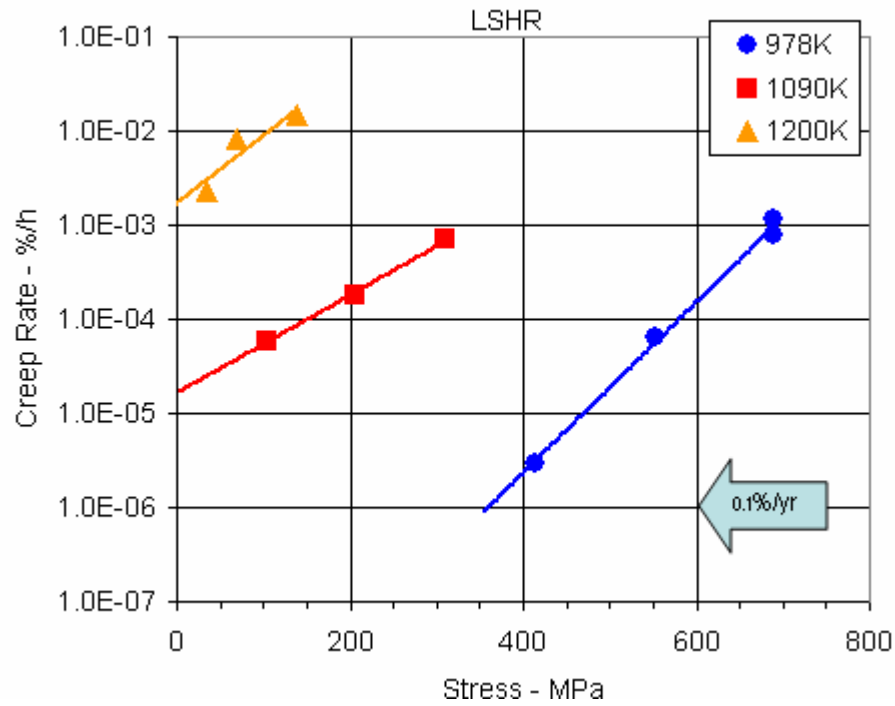


Figure 10.—Creep rate versus stress for LSHR.

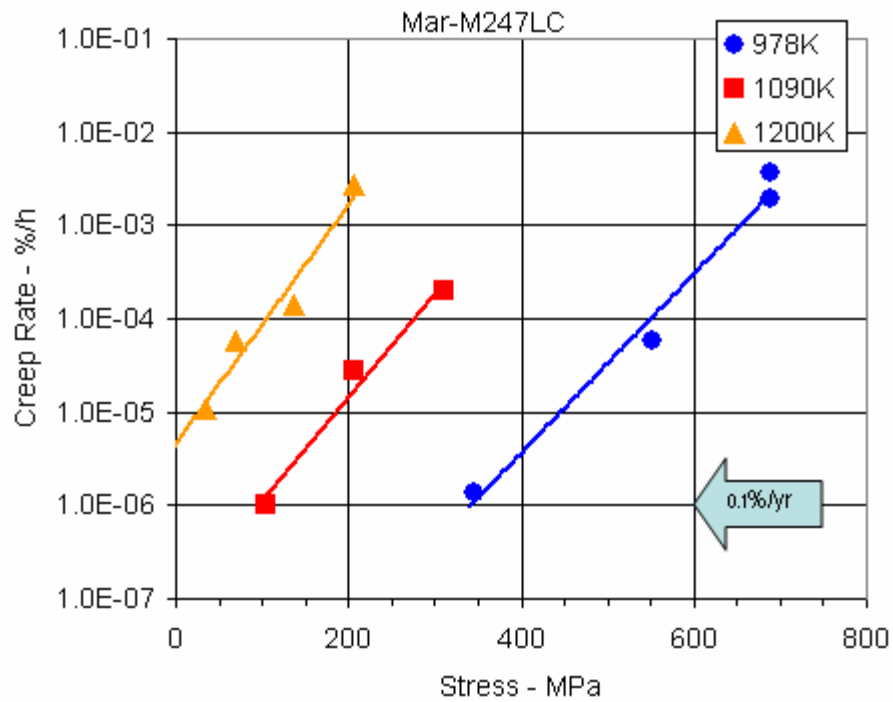


Figure 11.—Creep rate versus stress for conventionally cast Mar-M247LC.

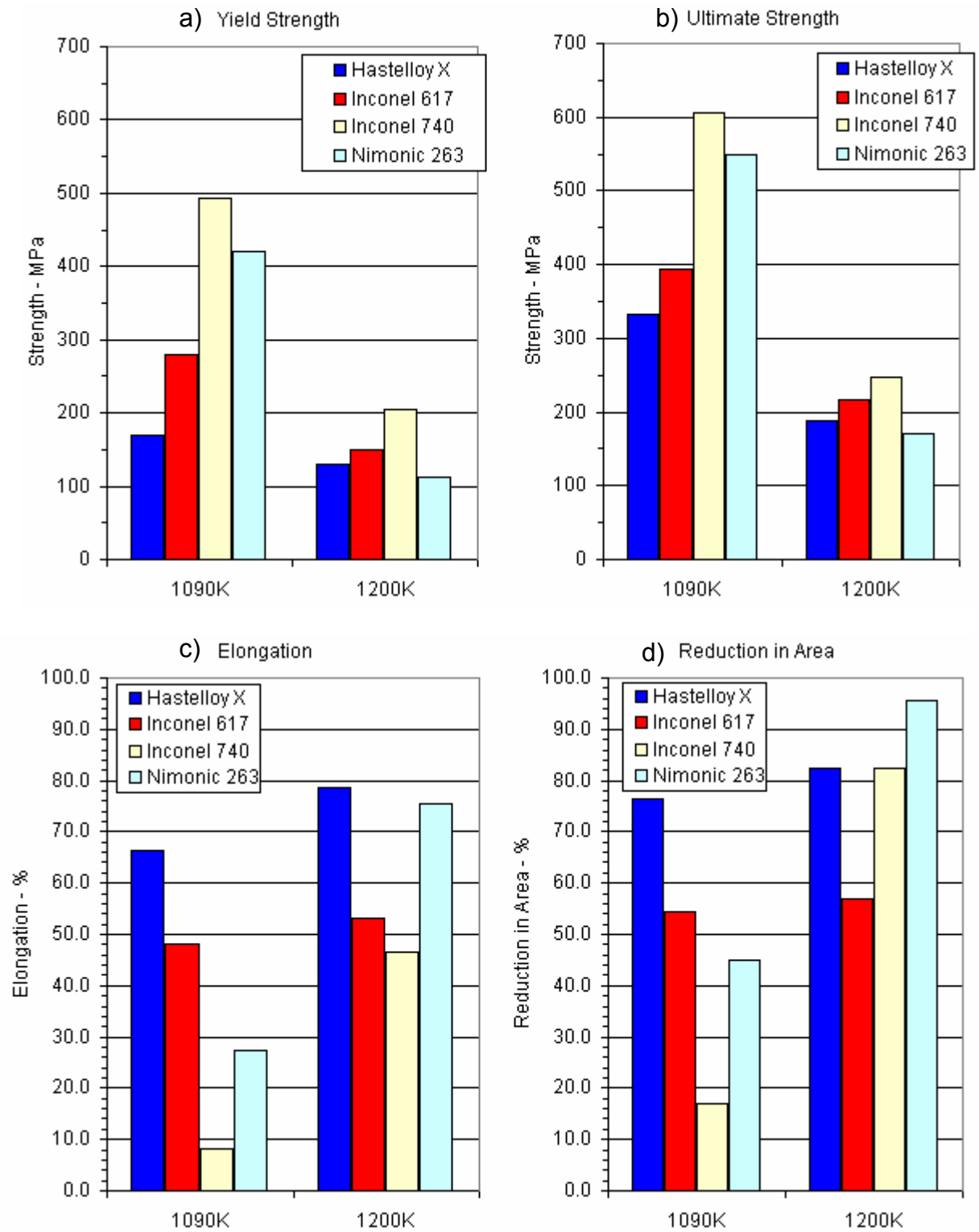


Figure 12.—Tensile response of selected duct alloys: a) yield strength, b) ultimate strength, c) elongation, d) reduction in area.

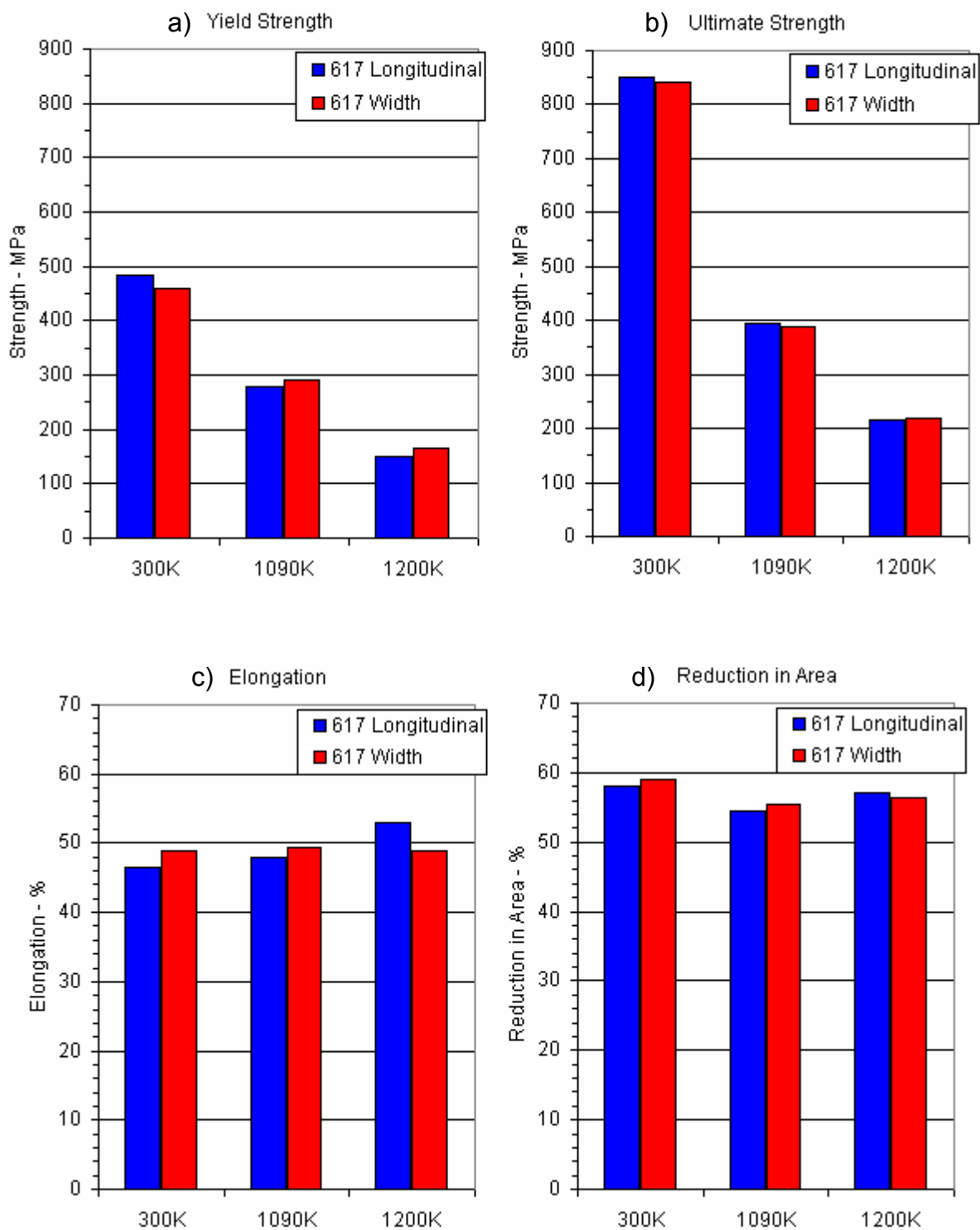


Figure 13.—Tensile response of Inconel 617 in plate longitudinal versus width directions:
a) yield strength, b) ultimate strength, c) elongation, d) reduction in area.

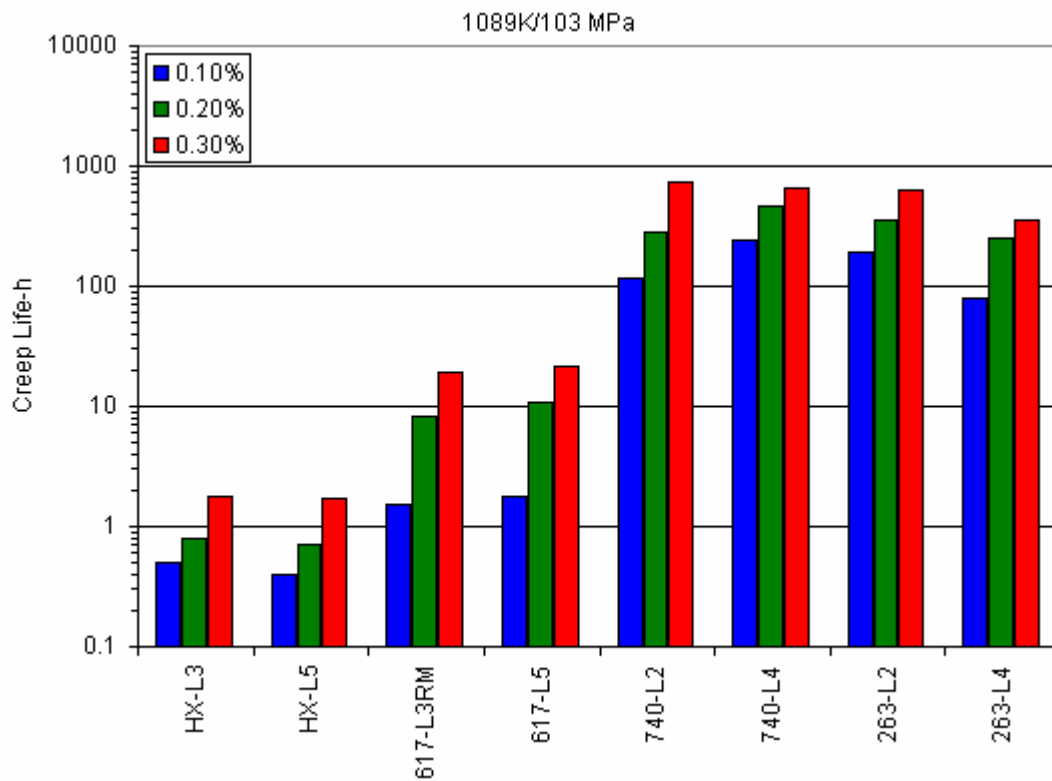


Figure 14.—Comparison of creep resistance for duct alloys at 1089K/103 MPa.

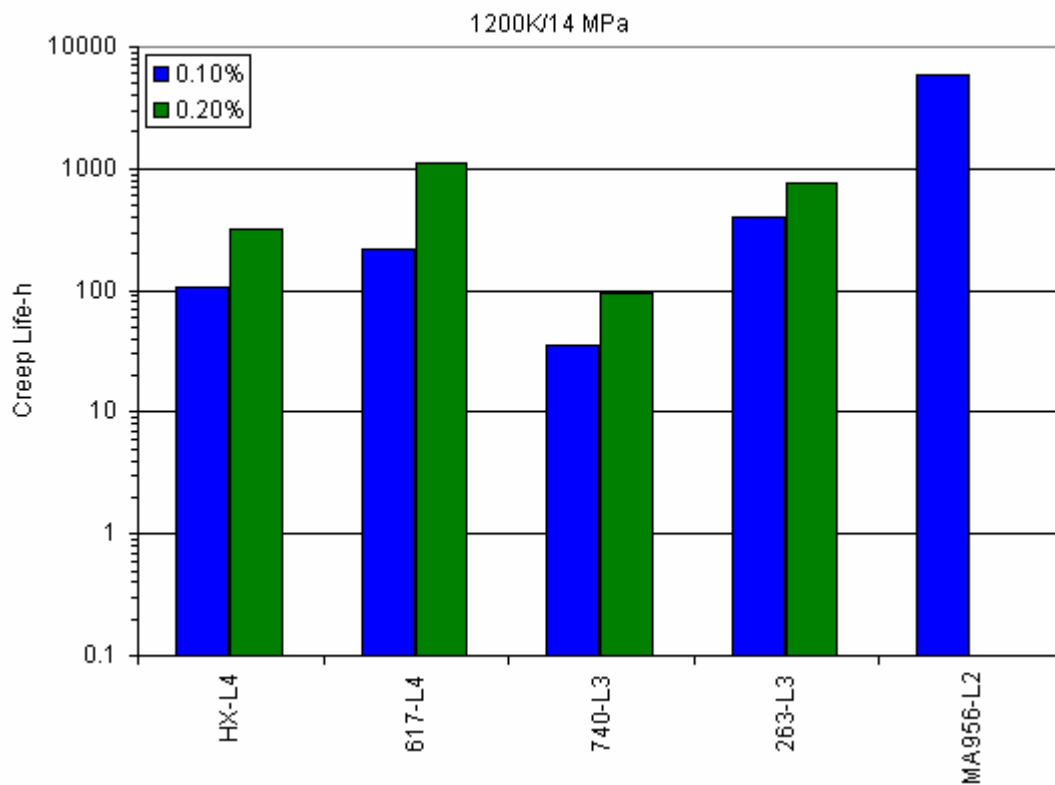


Figure 15.—Comparison of creep resistance for duct alloys at 1200K/14 MPa.

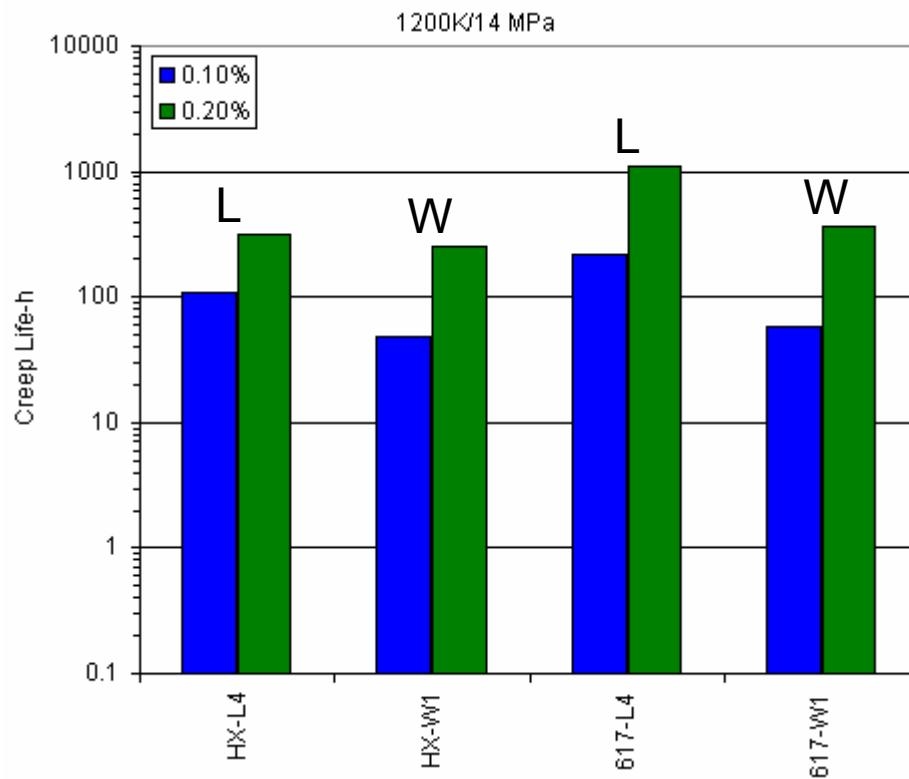


Figure 16.—Comparison of creep resistance of duct alloys Hastelloy X and Inconel 617 in the plate longitudinal and width directions at 1200K/14 MPa.

REPORT DOCUMENTATION PAGE			Form Approved OMB No. 0704-0188	
Public reporting burden for this collection of information is estimated to average 1 hour per response, including the time for reviewing instructions, searching existing data sources, gathering and maintaining the data needed, and completing and reviewing the collection of information. Send comments regarding this burden estimate or any other aspect of this collection of information, including suggestions for reducing this burden, to Washington Headquarters Services, Directorate for Information Operations and Reports, 1215 Jefferson Davis Highway, Suite 1204, Arlington, VA 22202-4302, and to the Office of Management and Budget, Paperwork Reduction Project (0704-0188), Washington, DC 20503.				
1. AGENCY USE ONLY (Leave blank)		2. REPORT DATE February 2006		3. REPORT TYPE AND DATES COVERED Technical Memorandum
4. TITLE AND SUBTITLE Tensile and Creep Property Characterization of Potential Brayton Cycle Impeller and Duct Materials			5. FUNDING NUMBERS WBS-22-973-80-50	
6. AUTHOR(S) Timothy P. Gabb and John Gayda				
7. PERFORMING ORGANIZATION NAME(S) AND ADDRESS(ES) National Aeronautics and Space Administration John H. Glenn Research Center at Lewis Field Cleveland, Ohio 44135-3191			8. PERFORMING ORGANIZATION REPORT NUMBER E-15444	
9. SPONSORING/MONITORING AGENCY NAME(S) AND ADDRESS(ES) National Aeronautics and Space Administration Washington, DC 20546-0001			10. SPONSORING/MONITORING AGENCY REPORT NUMBER NASA TM-2006-214110	
11. SUPPLEMENTARY NOTES Responsible person, Timothy P. Gabb, organization code RXA, 216-433-3272.				
12a. DISTRIBUTION/AVAILABILITY STATEMENT Unclassified - Unlimited Subject Category: 26 Available electronically at http://gltrs.grc.nasa.gov This publication is available from the NASA Center for AeroSpace Information, 301-621-0390.			12b. DISTRIBUTION CODE	
13. ABSTRACT (Maximum 200 words) This paper represents a status report documenting the work on creep of superalloys performed under Project Prometheus. Cast superalloys have potential applications in space as impellers within closed-loop Brayton cycle nuclear power generation systems. Likewise wrought superalloys are good candidates for ducts and heat exchangers transporting the inert working gas in a Brayton-based power plant. Two cast superalloys, Mar-M247LC and IN792, and a NASA GRC powder metallurgy superalloy, LSHR, are being screened to compare their respective capabilities for impeller applications. Several wrought superalloys including Hastelloy X, (Haynes International, Inc., Kokomo, IN), Inconel 617, Inconel 740, Nimonic 263, and Incoloy MA956 (Special Metals Corporation, Huntington, WV) are also being screened to compare their capabilities for duct applications. These proposed applications would require sufficient strength and creep resistance for long term service at temperatures up to 1200 K, with service times to 100,000 h or more. Conventional tensile and creep tests were performed at temperatures up to 1200 K on specimens extracted from the materials. Initial microstructure evaluations were also undertaken.				
14. SUBJECT TERMS Superalloys; Rotating impellers; Creep			15. NUMBER OF PAGES 30	
			16. PRICE CODE	
17. SECURITY CLASSIFICATION OF REPORT Unclassified	18. SECURITY CLASSIFICATION OF THIS PAGE Unclassified	19. SECURITY CLASSIFICATION OF ABSTRACT Unclassified	20. LIMITATION OF ABSTRACT	

